



# Structural basis for the specific recognition of IL-18 by its alpha receptor



Hui Wei<sup>a,b</sup>, Dongli Wang<sup>a,b</sup>, Yun Qian<sup>a,b</sup>, Xi Liu<sup>a,b</sup>, Shilong Fan<sup>a</sup>, Hsien-Sheng Yin<sup>c</sup>, Xinquan Wang<sup>a,b,\*</sup>

<sup>a</sup> Ministry of Education Key Laboratory of Protein Science, Center for Structural Biology, Collaborative Innovation Center for Biotherapy, School of Life Sciences, Tsinghua University, Beijing 100084, China

<sup>b</sup> Collaborative Innovation Center for Biotherapy, State Key Laboratory of Biotherapy and Cancer Center, West China Hospital, West China Medical School, Sichuan University, Chengdu, China

<sup>c</sup> Institute of Bioinformatics and Structural Biology, National Tsing Hua University, Hsinchu, Taiwan

## ARTICLE INFO

### Article history:

Received 16 June 2014

Revised 29 August 2014

Accepted 14 September 2014

Available online 26 September 2014

Edited by Stuart Ferguson

### Keywords:

Interleukin 18

Interleukin 18 receptor

Ligand-receptor recognition

X-ray structure

## ABSTRACT

**Interleukin 18 (IL-18), a member of the IL-1 family of cytokines, is an important regulator of innate and acquired immune responses. It signals through its ligand-binding primary receptor IL-18R $\alpha$  and accessory receptor IL-18R $\beta$ . Here we report the crystal structure of IL-18 with the ectodomain of IL-18R $\alpha$ , which reveals the structural basis for their specific recognition. It confirms that surface charge complementarity determines the ligand-binding specificity of primary receptors in the IL-1 receptor family. We suggest that IL-18 signaling complex adopts an architecture similar to other agonistic cytokines and propose a general ligand-receptor assembly and activation model for the IL-1 family.**

### Structured summary of protein interactions:

IL-18 and IL-18R alpha bind by x-ray crystallography (View interaction)

IL-18R alpha and IL-18 bind by molecular sieving (View interaction)

© 2014 Federation of European Biochemical Societies. Published by Elsevier B.V. All rights reserved.

## 1. Introduction

Interleukin 18 (IL-18) is an important cytokine participating in the regulation of innate and acquired immune responses [1–3]. Pleiotropic effects of IL-18, especially the induction of IFN- $\gamma$  from T cells and natural killer cells in synergy with IL-12 [4,5], are essential for immunity against invading pathogens [6]. However, the overproduction of IL-18 has been implicated in several autoimmune and chronic inflammatory disorders including rheumatoid arthritis, system lupus erythematosus, psoriasis, and inflammatory bowel disease in experimental animal models and clinical situations [7–9].

IL-18 is a member of the IL-1 family because of its structural homology, receptor utilization, signal transduction pathways, and biological effects [10]. IL-18 production has been detected from a variety of immune and non-immune cells including monocytes, macrophages, dendritic cells, epithelial cells, keratinocytes, and synovial fibroblasts [3]. Similar to IL-1 $\beta$ , IL-18 is first synthesized as a 23kDa inactive precursor (pro-IL-18), which is cleaved by caspase-1 to release the 18kDa active mature protein [2]. IL-18 binds to the IL-18 receptor alpha chain (IL-18R $\alpha$ ) and IL-18 receptor beta

chain (IL-18R $\beta$ ) on the surface of target cells to activate downstream NF- $\kappa$ B and MAPK pathways, which induce a variety of inflammatory cytokines [11]. IL-18R $\alpha$  is the primary receptor responsible for specific binding of IL-18, whereas IL-18R $\beta$ , an accessory co-receptor, does not directly bind to IL-18 but is required for signaling. Both receptors are members of the IL-1 receptor family, with an extracellular domain comprising three Ig-like domains, a transmembrane helix, and an intracellular Toll-IL-1R (TIR) domain responsible for signal transduction [11].

The agonistic cytokines in the IL-1 family include IL-1 $\alpha$ , IL-1 $\beta$ , IL-18, IL-33, IL-36 $\alpha$ , IL-36 $\beta$ , and IL-36 $\gamma$  [10]. IL-18 has its own specific co-receptor IL-18R $\beta$ , whereas others all use IL-1 receptor accessory protein (IL-1RACp) as the co-receptor in their respective signaling complexes. Our and other groups have revealed the structural basis for the interactions of IL-1 $\beta$  and IL-33 with their respective primary receptor and co-receptor IL-1RACp [12–14], which helps establish a stepwise ligand-receptor assembly and activation model for the IL-1RACp-dependent cytokines [13]. In this model, ligand recognition relies on the interaction of cytokine with its primary receptor: IL-1 $\alpha$  and IL-1 $\beta$  with IL-1RI, IL-33 with ST2, and IL-36 $\alpha$ , IL-36 $\beta$ , and IL-36 $\gamma$  with IL-1Rrp2. The binding of cytokine with primary receptor forms a composite surface to recruit IL-1RACp to form the ternary signaling complex [13]. Crystal structures of IL-18 with its receptors have not been reported. Therefore, the structural basis for the specific recognition of IL-18

\* Corresponding author at: Medical Science Building C226, Tsinghua University, Beijing 100084, China.

E-mail address: [xinquanwang@mail.tsinghua.edu.cn](mailto:xinquanwang@mail.tsinghua.edu.cn) (X. Wang).

by IL-18R $\alpha$  remains elusive. It is also unknown whether the assembly of IL-18R $\beta$  in the IL-18 signaling complex is similar to the assembly of IL-1RacP in the signaling complexes of other agonistic cytokines. To answer these questions and gain a complete understanding of ligand-receptor interaction and activation in the IL-1 family, we determined the crystal structure of human IL-18 in complex with the ectodomain of IL-18R $\alpha$ .

## 2. Materials and methods

### 2.1. Gene cloning, protein expression and purification

The cDNA encoding pro-IL-18 with four Cys mutated to Ser was cloned into pGEX-6p-1 vector with an N-terminal GST tag. The GST-pro-IL-18 fusion protein was expressed in *Escherichia coli* BL21 (DE3) by induction with 0.5 mM IPTG at 0.6–0.8 OD<sub>600</sub> in overnight cultures grown at 289 K. The cells were harvested by centrifugation and suspended with lysis buffer containing 50 mM Tris, pH 8.0, and 500 mM NaCl. After sonication, the lysate was centrifuged at 13 000 rpm for 1 h, and the supernatant was transferred to Glutathione Sepharose 4B column. After extensive wash of column with lysis buffer, the bound GST-pro-IL-18 was digested on column with caspase-1 overnight at 277 K. The released mature IL-18 was collected and further purified by gel-filtration chromatography using the Superdex 200 High Performance column (GE Healthcare) and the running buffer was the same as lysis buffer.

The ectodomain of IL-18R $\alpha$  (residues 19–329) was expressed in *Spodoptera frugiperda* Sf9 insect cells by using the Bac-to-Bac baculovirus expression system (Invitrogen). Sf9 insect cells were maintained in Insect-Xpress protein-free medium (Lonza) without serum at 300 K. The cDNA encoding the IL-18R $\alpha$  ectodomain was cloned into pFastBac vector with an N-terminal gp67 signal peptide to facilitate secretion and a C-terminal His-tag to facilitate purification. The plasmid was transformed into bacterial DH10Bac competent cells, and the extracted bacmid was transfected into Sf9 cells in the presence of Cellfectin II reagent (Invitrogen). After incubation of the transfected cells at 300 K for 7 d, the low-titer baculoviruses were harvested by collecting the supernatant of cell culture with centrifugation at 2000 rpm for 10 min. After two rounds of amplification, the high-titer viruses were used to infect Sf9 cells at a density of  $2 \times 10^6$  cells per milliliter. The supernatant of cell culture containing the IL-18R $\alpha$  ectodomain was harvested 60 h after infection, and concentrated and buffer-exchanged to HBS buffer containing 10 mM HEPES, pH 7.2, and 150 mM NaCl. The IL-18R $\alpha$  ectodomain was captured with nickel-beads, eluted with 500 mM imidazole in HBS buffer, and purified by gel-filtration chromatography using the Superdex 200 High Performance column (GE Healthcare) with the HBS running buffer. The purified IL-18R $\alpha$  ectodomain was digested with Endoglycosidase H and F1 at room temperature overnight and further purified by gel-filtration chromatography. To obtain the IL-18-IL-18R $\alpha$  binary complex, purified IL-18 and IL-18R $\alpha$  ectodomain were mixed on ice for 1 h and purified by gel-filtration chromatography using the Superdex 200 High Performance column (GE Healthcare) with the HBS running buffer.

### 2.2. Crystallization and data collection

The crystals of IL-18-IL-18R $\alpha$  complex were grown at 291 K by vapor diffusion in sitting drops composed of equal volumes of protein solution (10 mg/mL in 10 mM HEPES, pH 7.2, and 150 mM NaCl) and reservoir solution (20% polyethylene glycol 3350, 0.03 M citric acid, 0.07 M Bis-Tris propane, pH 7.6). All crystals were cryoprotected by soaking in reservoir solution supplemented with 20% glycerol for several seconds and then cooled in liquid

nitrogen. Diffraction data were collected on beam line BL17U at the Shanghai Synchrotron Research Facility (SSRF) and processed with HKL2000 [15].

### 2.3. Structure determination and refinement

A molecular replacement solution of IL-18 was determined with the program PHASER using the IL-18 NMR solution structure (PDB code 1J0S) as the search model [16,17]. The positions of the D1D2 module and D3 domain of IL-18R $\alpha$  were also determined with the program PHASER using the D1D2 module and D3 domain of IL-1RI (PDB code 1ITB) as search models [17,18]. There are two IL-18-IL-18R $\alpha$  complexes in the asymmetric unit, and non-crystallographic symmetry restraints were used in the subsequent structural refinement. Iterative refinement with the program PHENIX and model building with the program COOT were conducted [19,20], yielding a final model with  $R_{\text{work}}$  of 23.3% and  $R_{\text{free}}$  of 28.2%. The quality of the model was validated with the program PROCHECK [21], and all structure figures were made with the program PYMOL [22].

## 3. Results and discussion

### 3.1. Overall structure

It has been reported that the N-terminal pro-peptide is essential for the correct folding of IL-18 expressed in bacteria to obtain full activity [23]. In previous studies, all Cys residues in IL-18 were mutated to Ala or Ser to prevent polymerization through the oxidation of surface-exposed Cys74 and Cys104, and these mutants retained the biological activities as wild type IL-18 [24,25]. Therefore, we first expressed and purified human pro-IL-18 (193 residues) with an N-terminal GST tag in bacteria, in which four Cys residues in the mature IL-18 region were mutated to Ser. The mature IL-18 was obtained by cleavage with caspase-1 to remove the 36-residue pro-peptide (Fig. S1A). The purified IL-18 (residues Tyr1-Asp157) bound to human IL-18R $\alpha$  ectodomain (residues Ala19-Arg329), which was expressed and purified from insect cells, to form the IL-18-IL-18R $\alpha$  complex (Fig. S1B). The crystal structure of the complex was determined by the molecular replacement method at a resolution of 2.8 Å (Table 1). The final model in the asymmetric unit contains two IL-18-IL-18R $\alpha$  complexes (Fig. S2A), with residues Tyr1-Asn155 in IL-18 and residues Ser21-Cys43, Thr51-Arg71, Arg75-Leu161, Pro169-Glu253, and Asn260-Asp318 in IL-18R $\alpha$ . The electron density map allows us to visualize N-acetyl-D-glucosamine (NAG) attached to residues Asn197, Asn203, Asn236, and Asn297 of IL-18R $\alpha$  (Fig. 1). Two complex structures in the asymmetric unit are very similar with a r.m.s. deviations of 0.33 Å for all 430 C  $\alpha$  atoms (Fig. S2B). Therefore, we use one IL-18-IL-18R $\alpha$  complex structure in the subsequent description and discussion.

IL-18R $\alpha$  has a curved shape with three Ig-like domains (D1 to D3) (Fig. 1). The D1 and D2 domains pack together to form a D1D2 module, to which the D3 domain is connected through a linker (Fig. 1). The overall architecture of IL-18R $\alpha$  is very similar to those of IL-1RI and ST2, especially at the D1D2 module (Fig. S3A). The D3 domain is more flexible in its position related to the D1D2 module (Fig. S3B), reflecting the intrinsic domain-level conformation flexibility of D3 in ligand binding by primary receptors [13].

IL-18 in the complex adopts a  $\beta$ -trefoil fold comprised of 12 anti-parallel  $\beta$ -strands that are arranged in a threefold symmetric pattern (Fig. 1). This fold is a conserved signature structure for all IL-1 family of cytokines in spite of their low sequence similarity in the range of 10–40% [26]. The solution structure of IL-18 has been determined by NMR method [16]. Its complex structures with

**Table 1**  
Crystallographic data collection and refinement statistics.

<i>Data collection</i>	
Beamline	SSRF BL17U
Wavelength	0.9796 Å
Space group	$P2_1$
Cell dimensions	
a, b, c (Å)	71.39, 85.60, 88.12
$\alpha, \beta, \gamma$ (°)	90, 97.60, 90
Resolution (Å)	50–2.80 (2.88–2.80)
$R_{\text{merge}}$ (%)	12.1 (61.3)
$I/\sigma I$	10.5 (2.4)
Completeness (%)	97.5 (99.0)
Redundancy	2.9 (3.0)
<i>Refinement</i>	
Resolution (Å)	38.9–2.80 (2.91–2.80)
No. Reflections	25300 (2684)
$R_{\text{work}}/R_{\text{free}}$ (%)	23.3/28.2
No. atoms	
Protein	6989
Glycan	112
<i>B-factors</i> (Å <sup>2</sup> )	
Protein	58.2
Glycan	54.8
r.m.s. deviations	
Bond lengths (Å)	0.013
Bond angles (°)	1.799
Ramachandran plot (%)	
Most favored	86.7
Additionally allowed	11.9
Generously allowed	1.3
Disallowed	0.1

$R_{\text{work}}$  and  $R_{\text{free}}$  are defined by  $R = \frac{\sum |hkl| |F_{\text{obs}}| - |F_{\text{calc}}|}{\sum |hkl| |F_{\text{obs}}|}$ , where  $h, k, l$  are the indices of the reflections (used in refinement for  $R_{\text{work}}$ ; 5%, not used in refinement for  $R_{\text{free}}$ ) and  $F_{\text{obs}}$  and  $F_{\text{calc}}$  are the structure factors, deduced from intensities and calculated from the model, respectively.

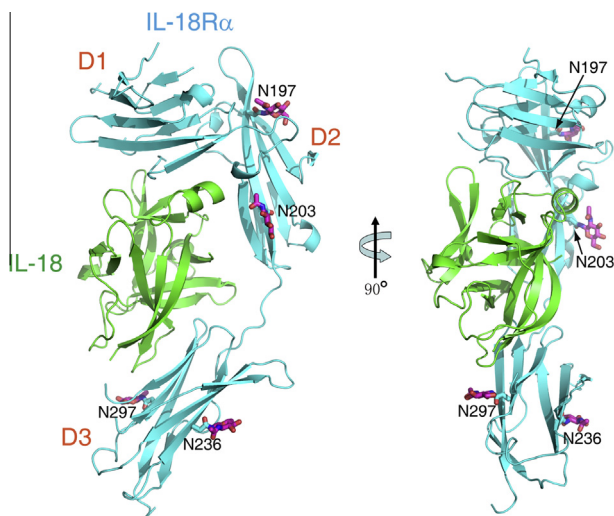


**Fig. 1.** Ribbon diagram of human IL-18 (green) in complex with the ectodomain of IL-18R $\alpha$  receptor (cyan). The observed NAGs linked to Asn197, Asn203, Asn236, and Asn297 of IL-18R $\alpha$  are colored in magenta.

an IL-18 neutralizing antibody 125-2H and the IL-18 binding protein (IL-18BP) have also been determined by X-ray crystallography, respectively [25,27]. Structural superimposition shows that the twelve  $\beta$ -strands forming the  $\beta$ -trefoil core of IL-18 are conserved in different states, whereas conformational variations reside in the loops connecting the strands, especially at the  $\beta$ 3– $\beta$ 4,  $\beta$ 4– $\beta$ 5, and  $\beta$ 11– $\beta$ 12 loops (Fig. S4). These loops are involved in the

interaction with receptors, and their roles will be described and discussed below.

### 3.2. Interactions between IL-18 and IL-18R $\alpha$

With the inner surface of the curved shape, IL-18R $\alpha$  binds IL-18 like a grasping hand with all three domains (Fig. 1). This binding mode has also been observed in the recognition of IL-1 $\beta$  by IL-1RI and IL-33 by ST2 (Fig. 2A) [13,14,18]. However, structural comparisons based on bound cytokine show that IL-18R $\alpha$  is tilted  $\sim 20^\circ$  from IL-1RI and ST2 in ligand binding (Fig. 2B).

The binding interface between IL-18 and IL-18R $\alpha$  is composed of two separate sites (Fig. 3). Site 1 between IL-18 and the D1D2 module of IL-18R $\alpha$  has a buried surface of  $\sim 845 \text{ \AA}^2$  (Fig. 3). Eleven IL-18 residues from  $\beta$ 1– $\beta$ 2 loop,  $\beta$ 2 and  $\beta$ 3 strands, and  $\beta$ 3– $\beta$ 4 and  $\beta$ 10– $\beta$ 11 loops interact with the D1D2 module of IL-18R $\alpha$  receptor with a 3.5 Å distance cutoff (Fig. S5). There is a significant conformational change in the  $\beta$ 3– $\beta$ 4 loop of IL-18 upon binding to IL-18R $\alpha$ . This loop extends away from the  $\beta$ -trefoil core in the solution structure of free IL-18, and it pulls inward by  $\sim 7 \text{ \AA}$  toward the core and has a short helix (Asp35–Asn41) when IL-18 binds to IL-18R $\alpha$  (Figs. S4 and S5). Most of IL-18 residues involved in the interaction with IL-18R $\alpha$ , including Glu31, Asp32, Met33, Thr34, Asp35, Asp37, Asp40, and Asn41, are adjacent to or in the helix (Fig. S5). Hydrophilic interactions between side chains of contacting residues dominate at site 1. These specific interactions include hydrogen bonds (Glu31–Ser24, Thr34–Gln124, Asp35–Ser127, and Asp40–Thr29) and salt bridges (Asp17–Lys128, Glu31–Arg25, and Asp37–Arg25) (Fig. 3). Site 2 between IL-18 and the D3 domain of IL-18R $\alpha$  is relatively smaller with a buried surface of  $\sim 603 \text{ \AA}^2$  (Fig. 3). Six IL-18 residues from  $\beta$ 4,  $\beta$ 5, and  $\beta$ 8 strands interact with the D3 domain of IL-18R $\alpha$  (Fig. S5). Hydrophobic IL-18 residue Met60 contacts with Ala301 of IL-18R $\alpha$ . IL-18 residue Lys53 forms a salt bridge with Glu253 of IL-18R $\alpha$  (Fig. 3). The NAG glycans linked to Asn197 and Asn236 of IL-18R $\alpha$  are far away from IL-18 ( $>15 \text{ \AA}$ ), whereas NAG glycans linked to Asn203 and Asn297 are much closer with a distance of  $\sim 4.5 \text{ \AA}$  to IL-18. The interactions observed at the interface are consistent with previous mutagenesis studies revealing that IL-18 residues Asp17, Met33, and Asp35 at site 1 and Lys53 and Met60 at site 2 are important for *in vitro* binding with IL-18R $\alpha$  and the activity to induce IFN- $\gamma$  [16,28,29].

IL-18 binding protein (IL-18BP) is a negative regulator of IL-18 signaling, which is not limited to just vertebrates, but also is encoded by many poxviruses to participate in viral immune evasion [2]. The ectromelia virus IL-18BP adopts a single Ig-fold and interacts with IL-18 in a manner very similar to the D3 domain of IL-18R $\alpha$  (Fig. S6) [27], therefore directly blocking the binding site 2 between IL-18 and IL-18R $\alpha$ .

### 3.3. Surface charge complementarity at site 1

Primary receptors IL-18R $\alpha$  and ST2 specifically recognize their respective ligands IL-18 and IL-33, whereas other primary receptors IL-1RI and IL-1Rrp2 show ligand-binding promiscuity. IL-1RI binds to agonistic IL-1 $\alpha$  and IL-1 $\beta$  and antagonistic IL-1Ra, and IL-1Rrp2 binds to agonistic IL-36 $\alpha$ , IL-36 $\beta$ , and IL-36 $\gamma$  [10]. Through studying the interaction of IL-33 with ST2, we previously found that site 1 between IL-33 and ST2 has specific salt-bridge interactions and surface charge complementarity, which are absent at site 1 between IL-1 $\alpha$  and IL-1RI and between IL-1 $\beta$  and IL-1RI [13]. This leads us to suggest that ST2 mainly uses surface charge complementarity at site 1 to achieve ligand-binding specificity [13]. At site 1 between IL-18 and IL-18R $\alpha$ , there is a continuous negative-charge patch on the surface of IL-18 formed by acidic Asp17, Glu31, Asp32, Asp35, Asp37, and Asp40 (Fig. 4). The corresponding positive-charge patch on the surface of IL-18R $\alpha$  D1D2

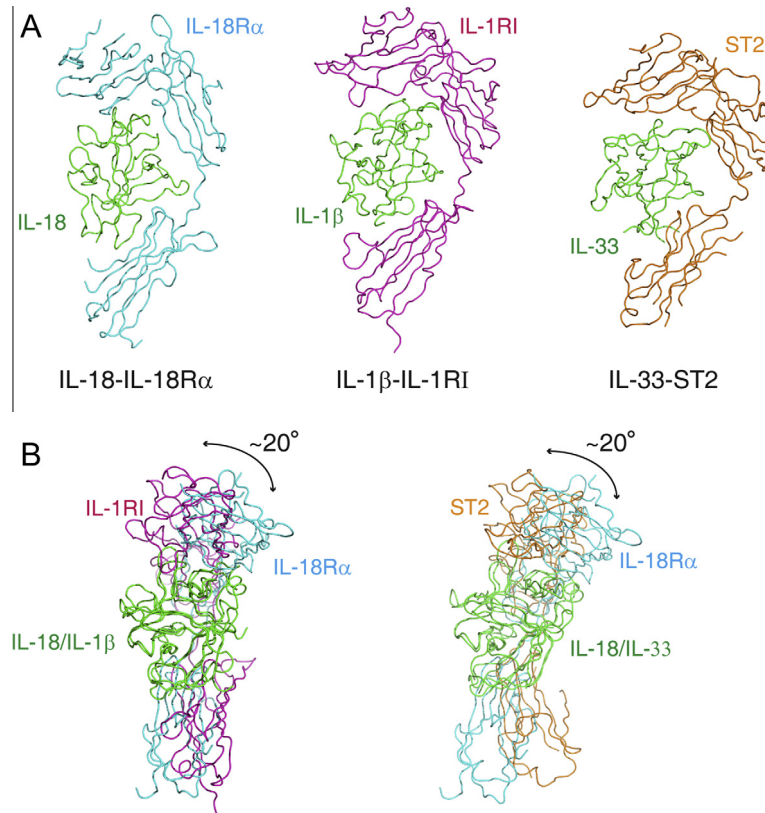


**Fig. 2.** The conserved binding mode between cytokine and primary receptor in the IL-1 family. (A) Structures of IL-18-IL-18R $\alpha$ , IL-1 $\beta$ -IL-1RI (PDB code 1ITB), and IL-33-ST2 (PDB code 4KC3) complexes. (B) Tilted IL-18R $\alpha$  (cyan) compared with IL-1RI (magenta) and ST2 (orange) when the structures are aligned based on bound cytokines.

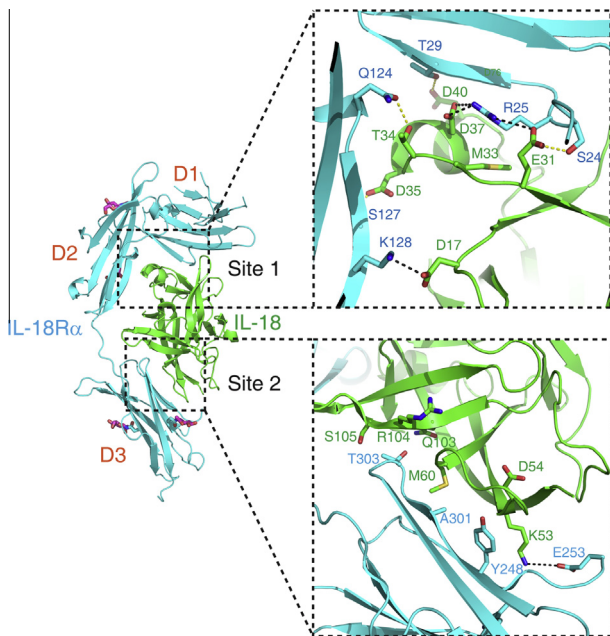


**Fig. 3.** The binding interface between IL-18 and IL-18R $\alpha$  is composed of two binding sites. Site 1 is between IL-18 and the D1D2 module of IL-18R $\alpha$ , and site 2 is between IL-18 and the D3 domain of IL-18R $\alpha$ . The zoom-in top panel shows the specific hydrogen-bonding (yellow dash lines) and salt-bridge (black dash lines) interactions between IL-18 and IL-18R $\alpha$  at site 1. The zoom-in bottom panel shows the hydrophobic and hydrophilic interactions at site 2. The Lys53-Glu253 salt bridge is represented with a black dash line.

module is formed by basic Arg25, His27, Arg123, and Lys128 (Fig. 4). Notably, IL-18 acidic residues Asp17 and Asp35 at site 1 are found to be important for the interaction with IL-18R $\alpha$  and the biological activities [16]. These results collectively indicate that surface charge complementarity at site 1 also determines the specific recognition of IL-18 by IL-18R $\alpha$ .

### 3.4. IL-18 signaling complex model

Through structural studies of IL-1 $\beta$  and IL-33 with their receptors [12,13], we found that the initial binding of IL-1RACp-dependent cytokines by their respective primary receptors generates a composite surface composed of the  $\beta$ 4- $\beta$ 5 and  $\beta$ 11- $\beta$ 12 loops of cytokine and the D2 domain of primary receptor to further recruit IL-1RACp to form the ternary signaling complex. However, IL-18 is the only agonistic cytokine in the IL-1 family that uses IL-18R $\beta$  instead of IL-1RACp as the signaling-essential co-receptor. How the IL-18R $\beta$  is recruited to form the IL-18 signaling complex is still not well understood in the absence of IL-18-IL-18R $\alpha$ -IL-18R $\beta$  complex structure. Here we show that the overall architecture of IL-18-IL-18R $\alpha$  is similar to the IL-1 $\beta$ -IL-1RI and IL-33-ST2 complexes that recruit IL-1RACp (Fig. 2A). This leads us to speculate that IL-18 signaling complex would adopt a similar architecture as IL-1 $\beta$  and IL-33 signaling complexes (Fig. 5A), in which the  $\beta$ 4- $\beta$ 5 and  $\beta$ 11- $\beta$ 12 loops of IL-18 are involved in the interaction with IL-18R $\beta$  (Fig. 5A).

IL-18-neutralizing monoclonal antibody 125-2H inhibits the binding of IL-18 to L428 cells that have expression of IL-18R $\alpha$  but low expression of IL-18R $\beta$  [30]. Antibody 125-2H binds to IL-18 with a large buried area of  $\sim$ 2350  $\text{Å}^2$ , which is at the high end

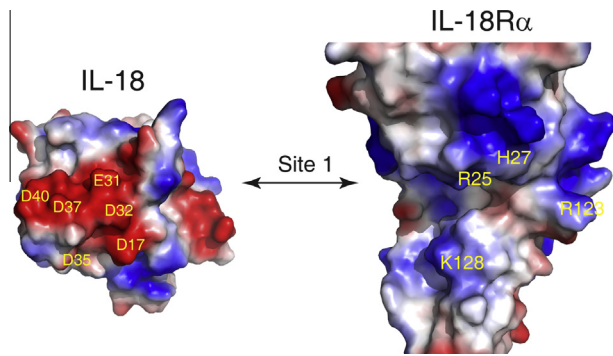


**Fig. 4.** Surface electrostatic potential of IL-18 and IL-18R $\alpha$  at binding site 1.

of antigen–antibody complexes [25]. The  $\beta 8$  strand,  $\beta 4$ – $\beta 5$ ,  $\beta 8$ – $\beta 9$ ,  $\beta 10$ – $\beta 11$ , and  $\beta 11$ – $\beta 12$  loops of IL-18 are involved in the interaction with 125-2H, among which the  $\beta 11$ – $\beta 12$  is the primary contacting loop containing anchor residue Leu144 (Fig. 5B) [25]. Structural superimposition shows that 125-2H and IL-18R $\alpha$  do have steric clashes between the D2 domain of IL-18R $\alpha$  and the V<sub>H</sub> domain of 125-2H heavy chain when they bind to IL-18 simultaneously (Fig. 5B), which explains the inhibition of IL-18 binding to L428 cells by 125-2H [30].

Interestingly, antibody 125-2H does not potently inhibit the binding of IL-18 to the TNF- $\alpha$ -primed KG-1 cells with high expression of IL-18R $\alpha$  and IL-18R $\beta$ , but it is still able to decrease the production of IFN- $\gamma$  by KG-1 cells stimulated by IL-18 [30]. It was proposed that the binding of IL-18R $\beta$  with IL-18 at site 3, which contains IL-18 residues Lys79, Lys84, and Asp98 [16], induces conformational changes of IL-18 and/or IL-18R $\alpha$  [25,30]. These changes presumably allow the binding of 125-2H to form

an antibody-IL-18-IL-18R $\alpha$ -IL-18R $\beta$  quaternary complex, however, the relative positional changes of IL-18 and its receptors after binding of 125-2H make the quaternary complex unable to induce downstream signaling as normal IL-18-IL-18R $\alpha$ -IL-18R $\beta$  ternary complex [25]. In our proposed IL-18-IL-18R $\alpha$ -IL-18R $\beta$  complex model, IL-18 interacts with IL-18R $\beta$  mainly through its  $\beta 4$ – $\beta 5$  and  $\beta 11$ – $\beta 12$  loops (Fig. 5A). Therefore, the binding site 3 between IL-18 and IL-18R $\beta$  in our proposed model is different from previously proposed one containing IL-18 residues Lys79, Lys84, and Asp98 [16]. Notably, the  $\beta 11$ – $\beta 12$  is also the primary loop for 125-2H interaction (Fig. 5B) [25]. Therefore, the formation of antibody-IL-18-IL-18R $\alpha$ -IL-18R $\beta$  quaternary complex in our model is unlikely. The IL-18R $\alpha$  and IL-18R $\beta$  heterodimers on TNF- $\alpha$ -primed KG-1 cells have much higher binding affinity for IL-18 than IL-18R $\alpha$  on L428 cells [30]. Therefore, the inhibition of 125-2H would be compromised in the binding of IL-18 to KG-1 cells than to L428 cells [30]. However, 125-2H would interfere with the stability of signaling-competent IL-18-IL-18R $\alpha$ -IL-18R $\beta$  complex by competing with IL-18 $\beta$ , thereby inhibiting the biological activity of IL-18 on TNF- $\alpha$ -primed KG-1 cells [30].

### 3.5. Ligand-receptor assembly and activation in the IL-1 family

Based on results from the current and previous studies [12–14,18], we suggest a general ligand-receptor assembly and activation model in the IL-1 family. The signaling depends on the recognition of cytokine by primary receptor and the subsequent recruitment of co-receptor IL-1RAcP or IL-18R $\beta$  (Fig. S7A). The signaling complexes in the IL-1 family adopt the “LEFT” architecture, in which co-receptor binds to the preformed cytokine and primary receptor from the left side, as seen from the concave surface of primary receptor (Fig. S7A).

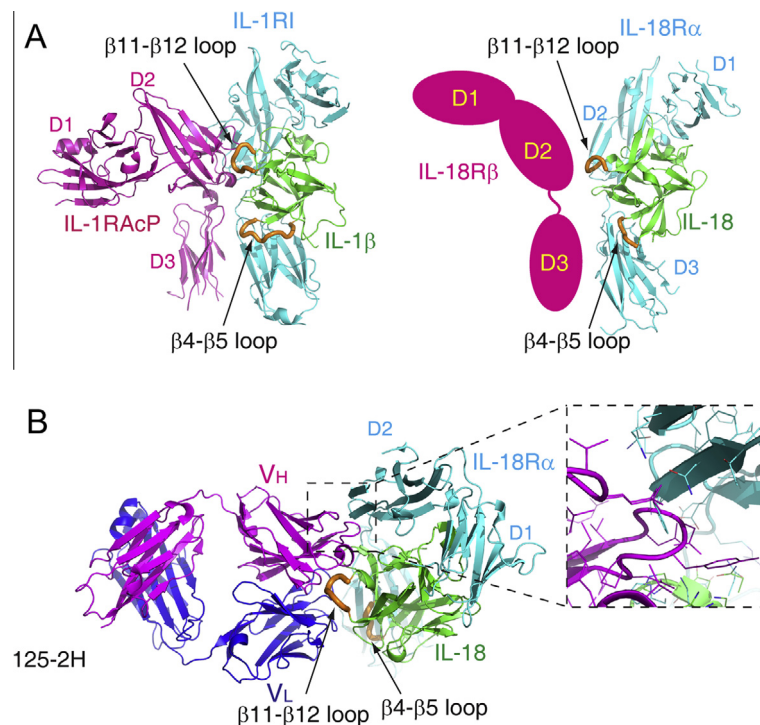


**Fig. 5.** IL-18-IL-18R $\alpha$ -IL-18R $\beta$  signaling complex model. (A) Left panel shows the structure of IL-1 $\beta$ -IL-1RI-IL-1RAcP ternary complex (PDB code 4DEP), in which the  $\beta 4$ – $\beta 5$  and  $\beta 11$ – $\beta 12$  loops of IL-1 $\beta$  interact with IL-1RAcP. Right panel shows a model of the IL-18-IL-18R $\alpha$ -IL-18R $\beta$  complex based on the determined IL-1 $\beta$ -IL-1RI-IL-1RAcP and IL-18-IL-18R $\alpha$  crystal structures. (B) Structural superimposition of IL-18-IL-18R $\alpha$  with IL-18-125-2H (PDB code 2VXT) structures. There are steric clashes between the D2 domain of IL-18R $\alpha$  and V<sub>H</sub> domain of 125-2H heavy chain, as shown in the zoom-in panel. The  $\beta 4$ – $\beta 5$  and  $\beta 11$ – $\beta 12$  we suggest to interact with IL-18R $\beta$  in the model are involved in the interaction with 125-2H.

The “LEFT” architecture is unique among various interleukins that utilize single-transmembrane cell-surface receptors to mediate their biological activities. The diverse members in the IL-1 family use the flexible loops in the  $\beta$ -trefoil fold to interact with the concave surface of their primary receptors, and the convex face of co-receptors IL-1RAcP or IL-18R $\beta$  is docked to the left side of the cytokine-primary receptor complex (Fig. S7A). Divergent helical interleukins with a helix-bundle core bind to receptors across the type I and type II divisions of the hematopoietic superfamily [31]. In contrast with the IL-1 family of cytokines, helical interleukins use the helices to interact with the convex face of both primary receptor and shared co-receptor such as common gamma chain and gp130 (Fig. S7B), focusing on the hinge region between two Ig-like domains [31]. The binding sites between helical interleukins and their receptors still have structural plasticity to accommodate sequence divergence and promiscuous interactions [31].

#### 4. Conclusions

In summary, we report the crystal structure of IL-18 bound to the ectodomain of IL-18R $\alpha$ . Analyses of binding interface, together with previous mutagenesis data, reveal critical residues for the specific recognition of IL-18 by IL-18R $\alpha$ . The structure also confirms that charge complementarity determines the ligand-binding specificity of primary receptors IL-18R $\alpha$  and ST2 in the IL-1 receptor family. We finally propose that IL-18 signaling complex adopts a “LEFT” architecture similar to the signaling complexes of IL-1RAcP-dependent cytokines. Therefore, a stepwise ligand-receptor assembly and activation model can be extended to include IL-18 with its specific receptors IL-18R $\alpha$  and IL-18R $\beta$ .

#### Acknowledgements

We thank assistance from Prof. J.H. He and the staff members at SSRF BL17U beam line with diffraction data collection. This work is supported by the Ministry of Science and Technology of China (2011CB910502 and 2010CB912402), Tsinghua University Initiative Scientific Program, and Toward World-Class University Project of National Tsing Hua University.

#### Appendix A. Supplementary data

Supplementary data associated with this article can be found, in the online version, at <http://dx.doi.org/10.1016/j.febslet.2014.09.019>.

#### References

- [1] Nakanishi, K., Yoshimoto, T., Tsutsui, H. and Okamura, H. (2001) Interleukin-18 regulates both Th1 and Th2 responses. *Annu. Rev. Immunol.* 19, 423–474.
- [2] Dinarello, C.A., Novick, D., Kim, S. and Kaplanski, G. (2013) Interleukin-18 and IL-18 Binding Protein. *Front. Immunol.* 4, 289.
- [3] Gracie, J.A., Robertson, S.E. and McInnes, I.B. (2003) Interleukin-18. *J. Leukoc. Biol.* 73, 213–224.
- [4] Nakamura, K., Okamura, H., Nagata, K., Komatsu, T. and Tamura, T. (1993) Purification of a factor which provides a costimulatory signal for gamma interferon production. *Infect. Immun.* 61, 64–70.
- [5] Okamura, H., Tsutsui, H., Komatsu, T., Yutsudo, M., Hakura, A., Tanimoto, T., Torigoe, K., Okura, T., Nukada, Y., Hattori, K., et al. (1995) Cloning of a new cytokine that induces IFN-gamma production by T cells. *Nature* 378, 88–91.
- [6] Dinarello, C.A. and Fantuzzi, G. (2003) Interleukin-18 and host defense against infection. *J. Infect. Dis.* 187 (Suppl. 2), S370–S384.
- [7] Boraschi, D. and Dinarello, C.A. (2006) IL-18 in autoimmunity: review. *Eur. Cytokine Netw.* 17, 224–252.
- [8] Sedimbi, S.K., Hagglof, T. and Karlsson, M.C. (2013) IL-18 in inflammatory and autoimmune disease. *Cell. Mol. Life Sci.* 70, 4795–4808.
- [9] Kanai, T., Kamada, N. and Hisamatsu, T. (2013) Clinical strategies for the blockade of IL-18 in inflammatory bowel diseases. *Curr. Drug Targets* 14, 1392–1399.
- [10] Garlanda, C., Dinarello, C.A. and Mantovani, A. (2013) The interleukin-1 family: back to the future. *Immunity* 39, 1003–1018.
- [11] Sims, J.E. (2002) IL-1 and IL-18 receptors, and their extended family. *Curr. Opin. Immunol.* 14, 117–122.
- [12] Wang, D., Zhang, S., Li, L., Liu, X., Mei, K. and Wang, X. (2010) Structural insights into the assembly and activation of IL-1 $\beta$  with its receptors. *Nat. Immunol.* 11, 905–911.
- [13] Liu, X., Hammel, M., He, Y., Tainer, J.A., Jeng, U.S., Zhang, L., Wang, S. and Wang, X. (2013) Structural insights into the interaction of IL-33 with its receptors. *Proc. Natl. Acad. Sci. USA* 110, 14918–14923.
- [14] Thomas, C., Bazan, J.F. and Garcia, K.C. (2012) Structure of the activating IL-1 receptor signaling complex. *Nat. Struct. Mol. Biol.* 19, 455–457.
- [15] Otwinowski, Z. and Minor, W. (1997) Processing of X-ray diffraction data collected in oscillation mode. *Method Enzymol.* 276, 307–326.
- [16] Kato, Z., Jee, J., Shikano, H., Mishima, M., Ohki, I., Ohnishi, H., Li, A., Hashimoto, K., Matsukuma, E., Omoya, K., et al. (2003) The structure and binding mode of interleukin-18. *Nat. Struct. Mol. Biol.* 10, 966–971.
- [17] McCoy, A.J., Grosse-Kunstleve, R.W., Adams, P.D., Winn, M.D., Storoni, L.C. and Read, R.J. (2007) Phaser crystallographic software. *J. Appl. Crystallogr.* 40, 658–674.
- [18] Vigers, G.P., Anderson, L.J., Caffes, P. and Brandhuber, B.J. (1997) Crystal structure of the type-I interleukin-1 receptor complexed with interleukin-1 $\beta$ . *Nature* 386, 190–194.
- [19] Adams, P.D., Grosse-Kunstleve, R.W., Hung, L.W., Ioerger, T.R., McCoy, A.J., Moriarty, N.W., Read, R.J., Sacchettini, J.C., Sauter, N.K. and Terwilliger, T.C. (2002) PHENIX: building new software for automated crystallographic structure determination. *Acta Crystallogr. D* 58, 1948–1954.
- [20] Emsley, P. and Cowtan, K. (2004) Coot: model-building tools for molecular graphics. *Acta Crystallogr. D* 60, 2126–2132.
- [21] Laskowski, R.A., MacArthur, M.W., Moss, D.S. and Thornton, J.M. (1993) PROCHECK: a program to check the stereochemical quality of protein structures. *J. Appl. Crystallogr.* 26, 283–291.
- [22] DeLano, W.L. (2002) Pymol Molecular Graphics System, DeLano Scientific, San Carlos, California, USA.
- [23] Liu, B., Novick, D., Kim, S.H. and Rubinstein, M. (2000) Production of a biologically active human interleukin 18 requires its prior synthesis as PRO-IL-18. *Cytokine* 12, 1519–1525.
- [24] Yamamoto, Y., Kato, Z., Matsukuma, E., Li, A., Omoya, K., Hashimoto, K., Ohnishi, H. and Kondo, N. (2004) Generation of highly stable IL-18 based on a ligand-receptor complex structure. *Biochem. Biophys. Res. Commun.* 317, 181–186.
- [25] Argiriadi, M.A., Xiang, T., Wu, C., Ghayur, T. and Borhani, D.W. (2009) Unusual water-mediated antigenic recognition of the proinflammatory cytokine interleukin-18. *J. Biol. Chem.* 284, 24478–24489.
- [26] Krumm, B., Xiang, Y. and Deng, J. (2014) Structural biology of the IL-1 superfamily: key cytokines in the regulation of immune and inflammatory responses. *Protein Sci.* 23, 526–538.
- [27] Krumm, B., Meng, X., Li, Y., Xiang, Y. and Deng, J. (2008) Structural basis for antagonism of human interleukin 18 by poxvirus interleukin 18-binding protein. *Proc. Natl. Acad. Sci. USA* 105, 20711–20715.
- [28] Kim, S.H., Azam, T., Novick, D., Yoon, D.Y., Reznikov, L.L., Buefler, P., Rubinstein, M. and Dinarello, C.A. (2002) Identification of amino acid residues critical for biological activity in human interleukin-18. *J. Biol. Chem.* 277, 10998–11003.
- [29] Meng, X., Leman, M. and Xiang, Y. (2007) Variola virus IL-18 binding protein interacts with three human IL-18 residues that are part of a binding site for human IL-18 receptor alpha subunit. *Virology* 358, 211–220.
- [30] Wu, C., Sakorafas, P., Miller, R., McCarthy, D., Scesney, S., Dixon, R. and Ghayur, T. (2003) IL-18 receptor beta-induced changes in the presentation of IL-18 binding sites affect ligand binding and signal transduction. *J. Immunol.* 170, 5571–5577.
- [31] Wang, X., Lupardus, P., Laporte, S.L. and Garcia, K.C. (2009) Structural biology of shared cytokine receptors. *Annu. Rev. Immunol.* 27, 29–60.